Novel Coarse Timing Synchronization Methods in OFDM Systems Using Fourth-Order Statistics

Ali Mohebbi, Hamed Abdzadeh-Ziabari, *Student Member, IEEE*, and Mahrokh G. Shayesteh, *Member, IEEE*

***Abstract*—In this paper, the problem of coarse timing synchronization in orthogonal frequency-division multiplexing (OFDM) systems is investigated, and two new timing metrics with better performance are presented. The new metrics take advantage of two novel differential normalization functions that are based on the fourth-order statistics and are designed depending on the value of carrier frequency offset (CFO). The proposed timing metrics are theoretically evaluated using two different class separability criteria. It is shown that the new schemes considerably increase the difference between the correct and wrong timing points in comparison with previous methods. The computational complexity of the new methods is obtained, and their superior detection performances are also demonstrated in terms of probabilities of false alarm and missed detection. The results indicate that due to a significant improvement in missed detection probability (MDP), the new methods offer a considerably wider range of acceptable thresholds.**

***Index Terms*—Differential normalization, fourth-order statistics, orthogonal frequency-division multiplexing (OFDM), preamble, timing synchronization.**

I. Introduction

As an effective multicarrier transmission technique, orthogonal frequency-division multiplexing (OFDM), due to its attractive features such as providing immunity to multipath fading and efficient hardware implementation [1], has been adopted in different digital communications systems such as wireless local area networks (WLANs), digital video broadcasting, and wireless metropolitan area networks.

The requirement of OFDM systems for synchronization has resulted in the proposition of different methods for timing and frequency offset estimation. For timing offset estimation, Schmidl and Cox in [2] proposed the use of correlation between the two identical parts of a preamble in the time domain. Later, in [3]–[5], the structure of the preamble was modified for having a timing metric with a sharper peak. A method similar to [2] was presented in [6] and analyzed in [7] for timing estimation utilizing the two identical parts of a preamble. In [8], Ruan *et al.* demonstrated that using more than one preamble, which is available in wireless systems such as WiMAX and WLAN, can improve timing estimation. Recently, in [9], a method has been proposed, which not only uses the correlation function presented in [2] but takes advantage of differential normalization as well. Normalization was traditionally used to enable the timing metric to avoid the fluctuations of the received signal power [8]. However, in [9], it is demonstrated that when the preamble is present, the difference between the two identical parts of the received signal reaches its minimum value, and if this difference value is applied to the normalization of the timing metric, it gives rise to a greater difference between the values of the timing metric at the correct and wrong timing points and, consequently, improves timing estimation performance. In the method presented in [9], instead of having a timing metric with the maximum value of 1 (as in the conventional schemes), the value of the timing metric at its maximum point is designed to be dependent on the signal-to-noise ratio (SNR). In another recent method [10], the important issue of sufficient statistics for timing estimation of a preamble composed of two identical parts in the time domain is addressed, and it is demonstrated that since sufficient statistics for timing estimation do not exist, there is no optimal method in the sense of using sufficient statistics. Therefore, it is possible to have a new method with better performance than the previous schemes. Moreover, in [10], the use of the fourth-order correlation function is proposed instead of the second-order correlation function utilized in the conventional methods.

In comparison with the aforementioned methods that use only the periodicity of the received preamble for correlation, there are also some schemes that take advantage of the samples of the pure preamble by using its cross-correlation with the received signal [11]–[13]. These methods need to know the exact preamble signal that may not be always feasible [14]. Furthermore, there are some methods that blindly estimate the start of frame using the characteristics of the cyclic prefix (CP) [15]–[18].

In [9] and [10], the performance evaluation of the timing metrics has been done by resorting to the class separability criterion. According to this criterion, the best timing metric (classifier) is that whose values at the two classes (the correct and wrong timing points) are more distinct than those of other metrics [19]. In other words, the main issue in designing a timing metric and estimating its performance is to select the features from the received signal that make the two classes as separate as possible [19].

Manuscript received June 22, 2013; revised November 27, 2013 and April 1, 2014; accepted June 26, 2014. Date of publication July 8, 2014; date of current version May 12, 2015. This work was supported by the Iran National Science Foundation (INSF) under Contract no. 91041042. The review of this paper was coordinated by Dr. X. Dong.

A. Mohebbi is with the Department of Electrical Engineering, Azad University, South Tehran Branch, Tehran 17776-13651, Iran (e-mail: ali.mohebbi@yahoo.com).

H. Abdzadeh-Ziabari was with the Department of Electrical Engineering, Urmia University, Urmia, Iran. He is currently with the Department of Electrical and Computer Engineering, Concordia University, Montreal, QC H3G 1M8, Canada (e-mail: h_abdza@encs.concordia.ca).

M. G. Shayesteh is with the Department of Electrical Engineering, Urmia University, Urmia 57561-15311, Iran. She is also working with the Wireless Research Laboratory, Advanced Communications Research Institute (ACRI), Department of Electrical Engineering, Sharif University of Technology, Tehran 11365-9363, Iran (e-mail: m.shayesteh@urmia.ac.ir).

Digital Object Identifier 10.1109/TVT.2014.2336754

0018-9545 © 2014 IEEE. Personal use is permitted, but republication/redistribution requires IEEE permission.
See http://www.ieee.org/publications_standards/publications/rights/index.html for more information.

In this paper, with the aim of increasing class separability, we propose two novel timing metrics. These metrics take advantage of the fourth-order correlation function along with the fourth-order differential normalization functions. The new differential normalization functions are made from the products of the second-order differential elements and are proposed for two cases: the presence of negligible carrier frequency offset (CFO) and nonnegligible CFO.

The class separability performances of the new methods are theoretically evaluated utilizing two criteria: 1) the mean values of the timing metrics and 2) both the mean and variance values of the timing metrics. It is shown that the new schemes considerably increase class separability. Hence, they offer remarkably better detection performances that are demonstrated using the probabilities of false alarm and missed detection. Furthermore, the computational complexity of the proposed normalization functions is investigated.

The rest of this paper is organized as follows. In Section II, we concisely describe an OFDM system along with some backgrounds on timing synchronization. Section III explains the proposed methods. Section IV is dedicated to the performance evaluation of the proposed methods and computational complexity comparisons. In Section V, the numerical results are presented, and finally, Section VI contains the concluding remarks.

II. System Description

Here, first, we briefly explain an OFDM system and then address the preamble-aided timing synchronization.

A. OFDM System Model

An OFDM system with N subcarriers is considered that uses a preamble composed of two identical parts in the time domain. The preamble samples in the frequency domain $S(n)$, $0 \le n \le N-1$ can be made of a pseudo-noise sequence for even subcarriers and a zero sequence for odd subcarriers. By taking the inverse discrete Fourier transform (which can be efficiently implemented using a fast-Fourier-transform algorithm) of $S(n)$, $0 \le n \le N-1$, and adding the CP, the transmitted signal in the time domain has the following form:

$$s(k) = \frac{1}{\sqrt{N}} \sum_{n=0}^{N-1} S(n) \exp\left(j2\pi k \frac{n}{N}\right), \quad -N_g \le k \le N-1 \tag{1}$$

where N_g is the CP length, and $s(k) = s(k + (N/2)), 0 \le k \le (N/2) - 1$. The transmitted signal passes through a frequency-selective fading channel with length L_h and impulse response $h(l),\ l = 0, 1, \ldots, L_h - 1$. Thus, the preamble signal at the receiver can be expressed as

$$r(k) = y(k) e^{j\frac{2\pi k}{N}\varepsilon} + w(k), \quad -N_g \le k \le N + L_h - 2 \tag{2}$$

where ε is the CFO normalized by the subcarrier spacing $1/T$ (T is an OFDM symbol interval), and $w(k)$ is a sample of complex additive white Gaussian noise with zero mean and variance σ_w^2. Furthermore, $y(k)$ is the response of the channel to the transmitted preamble, which is defined as

$$y(k) = \sum_{l=0}^{L_h-1} h(l) s(k-l), \quad -N_g \le k \le N + L_h - 2. \tag{3}$$

It is worth mentioning that the preamble consisting of two identical parts in the time domain remains periodic after passing through a multipath channel as long as the length of each part is greater than the delay spread of the channel. Therefore, we have $y(k) = y\left(k + (N/2)\right), -N_g + L_h \le k \le N - 1$.

B. Timing Synchronization

The aim of timing synchronization in OFDM systems is to find the start of frame, which is usually achieved by using a preamble with two identical parts in the time domain in practical systems such as WLAN and WiMAX [20]. The work of Ruan *et al.* [8], similar to that of Schmidl and Cox [2], utilized the correlation between the two identical parts as

$$P_R(d) = \sum_{k=0}^{(N/2)-1} r^*(d+k) r\left(d+k+(N/2)\right) \tag{4}$$

(where "$*$" denotes the complex conjugate operator) and proposed the following timing metric to estimate the start of frame:

$$T_R(d) = 2\frac{|P_R(d)|}{R_R(d)} \tag{5}$$

where

$$R_R(d) = \sum_{k=0}^{N-1} |r(d+k)|^2 \tag{6}$$

is the normalization function. The normalization function is used to avoid the harmful effects of power fluctuations of the received signal [8] so that when the preamble is present $(d = d_{\rm pr})$, the timing metric has the mean value $E\{T_R(d_{\rm pr})\} = 1/[1 + (1/\mathrm{SNR})]$, which, for high SNRs, is approximately equal to $E\{T_R(d_{\rm pr})\} \approx 1$, where $\mathrm{SNR} = \sigma_y^2/\sigma_w^2$, $\sigma_y^2 = E\{|y(k)|^2\}$, and $E\{\cdot\}$ denotes the expectation operator.

In [9], Zhang and Huang proposed differential normalization functions to improve the timing synchronization performance. The timing metric $T_Z(d) = |P_R(d)|/R_Z(d)$ proposed in [9] utilizes the same correlation function as (4) but takes advantage of two differential normalization functions, namely, magnitude of difference (MoD) $R_{Z,\mathrm{MoD}}(d)$ and difference of magnitude (DoM) $R_{Z,\mathrm{DoM}}(d)$, that are, respectively, defined as follows:

$$R_{Z,\,\mathrm{MoD}}(d) \triangleq \sum_{k=0}^{(N/2)-1} |r(d+k) - r\left(d+k+(N/2)\right)|^2 \tag{7}$$

$$R_{Z,\,\mathrm{DoM}}(d) \triangleq \sum_{k=0}^{(N/2)-1} \left(|r(d+k)| - |r\left(d+k+(N/2)\right)|\right)^2. \tag{8}$$

$R_{Z,\mathrm{DoM}}(d)$ is robust to CFO, whereas $R_{Z,\mathrm{MoD}}(d)$ can only be applied when the CFO is negligible. The timing metric proposed in [9] avoids power fluctuations by making the maximum value of the timing metric dependent on SNR. For fixed values of SNR, the timing metric in [9] produces the same values on average, and therefore, power fluctuations are avoided. As an example, the timing metric utilizing MoD, in the presence of the preamble and for small values of CFO, has the mean value $E\{T_{Z,\mathrm{MoD}}(d_{\mathrm{pr}})\} \approx \mathrm{SNR}/2$. Owing to differential normalization, the metrics in [9] have sharper peaks and lower probabilities of false alarm and missed detection compared with those in [8].

Abdzadeh-Ziabari and Shayesteh in [10] demonstrated that sufficient statistics for timing synchronization of a preamble with two identical parts in the time domain do not exist, and there is no optimal method in the sense of using sufficient statistics. This important fact is the motivation for proposing new schemes in the following section to improve the performance of timing synchronization.

III. Proposed Methods

The design of a timing metric as a feature selection problem mainly deals with the following issue: What features from the received signal should be utilized to make the values of the timing metric at the correct and wrong timing points as different as possible? Here, considering the given issue, we propose two new timing metrics.

A. Double Differential Normalization (DDN)

To disclose the idea behind the first proposed method, we consider the second-order timing metric presented in [9]. This metric takes advantage of the second-order correlation in (4), i.e., $(\sum_{k=0}^{(N/2)-1} r^*(d+k)r(d+k+(N/2)))$, along with the second-order differential normalization in (7). The MoD normalization function presented in [9] obtains the energy of a vector that is constructed from the difference between the elements of the received signal as follows:

$$\Delta^{\mathrm{MoD},d} = \left\{ \begin{array}{l} \underbrace{|r(d) - r\left(d+(N/2)\right)|}_{\Delta^{\mathrm{MoD},d}(0)}, \\ \underbrace{|r(d+1) - r\left(d+(N/2)+1\right)|}_{\Delta^{\mathrm{MoD},d}(1)}, \\ \cdots, \\ \underbrace{|r\left(d+(N/2)-1\right) - r(d+N-1)|}_{\Delta^{\mathrm{MoD},d}((N/2)-1)} \end{array} \right\}. \quad (9)$$

The use of this vector in [9] relies on the idea that when the preamble consisting of two identical parts is received, the difference between the samples of the received signal, i.e., $|r(k) - r(k+(N/2))|^2$, decreases. Thus, the value of the normalization function in (7), i.e., the sum $R_{Z,\mathrm{MoD}}(d) \triangleq \sum_{k=0}^{(N/2)-1} |r(d+k) - r(d+k+(N/2))|^2$, significantly decreases in comparison with the conventional normalization function $R_R(d) = \sum_{k=0}^{N-1} |r(d+k)|^2$ in [8]. Hence, at the correct timing point, the value of the timing metric $T_{Z,\mathrm{MoD}}(d) = |P_R(d)|/R_{Z,\mathrm{MoD}}(d)$ in [9] significantly increases in comparison with the conventional metrics $T_R(d) = 2|P_R(d)|/R_R(d)$ in [8]. By this means, the difference between the values of the metric at the correct and wrong timing points increases, and the timing metric becomes sharper.

In this paper, to have a timing metric whose values at the correct and wrong timing points are more distinct, instead of using the second-order elements $r^*(k)r(k+(N/2))$ for correlation along with the difference $|r(k) - r(k+(N/2))|^2$ for normalization, we propose to use the fourth-order elements (for example, $r^*(k)r^*(k+1)r(k+(N/2))r(k+(N/2)+1)$) for correlation and the product of the differences (for example, $|r(k) - r(k+(N/2))|^2|r(k+1) - r(k+(N/2)+1)|^2$, which are of fourth order) for normalization. At the presence of a preamble with two identical parts, the fourth-order correlation function along with the fourth-order normalization function produce a peak in timing metric, which is significantly greater than the previous methods. Hence, the new method has values with greater difference at the correct and wrong timing instants, compared with the existing methods (the mathematical justification of this statement will be given in the following section).

Therefore, the proposed timing metric has the following form:

$$T^{\mathrm{new}}(d) = \frac{|P(d)|}{R(d)} \quad (10)$$

where $P(d)$ is the fourth-order correlation function, and $R(d)$ is the fourth-order differential normalization function. The fourth-order correlation function that we use has the following form [10]:

$$\begin{aligned} P(d) = \sum_{l=1}^{a}\sum_{k=0}^{b} & \left(r^*(k+d)r^*(k+d+l)r\left(k+d+(N/2)\right)\right. \\ & \left.\times r\left(k+d+l+(N/2)\right)\right), \\ & 1 \le a \le (N/2)-1,\ 0 \le b \le (N/2)-a-1 \end{aligned} \quad (11)$$

where a and b are the parameters that determine the correlation length L (where $L \le (N/4)((N/2)-1)$), which are designed based on the desired performance [10]. Now, for the fourth-order correlation function, we present a new fourth-order differential normalization function $R(d) = R^{\mathrm{DDN}}(d)$.

For the new differential normalization function, instead of using $\Delta^{\mathrm{MoD},d}$ in (9), we propose to build a new vector $\mathbf{Q}^{\mathrm{DDN},d}$ whose elements are derived from the multiplication of the elements of (9) in the following way:

$$\begin{aligned} \mathbf{Q}^{\mathrm{DDN},d} = \Bigg\{ & \underbrace{|r(d) - r\left(d+(N/2)\right)|}_{\Delta^{\mathrm{MoD},d}(0)} \\ & \times \underbrace{|r(d+1) - r\left(d+(N/2)+1\right)|}_{\Delta^{\mathrm{MoD},d}(1)}, \\ & \underbrace{|r(d) - r\left(d+(N/2)\right)|}_{\Delta^{\mathrm{MoD},d}(0)} \end{aligned}$$

$$\times \underbrace{|r(d+2)-r\left(d+(N/2)+2\right)|}_{\Delta^{\mathrm{MoD},d}(2)},$$

$$\cdots,$$

$$\underbrace{|r(d)-r\left(d+(N/2)\right)|}_{\Delta^{\mathrm{MoD},d}(0)}$$
$$\times \underbrace{|r\left(d+(N/2)-1\right)-r(d+N-1)|}_{\Delta^{\mathrm{MoD},d}((N/2)-1)},$$
$$\underbrace{|r(d+1)-r\left(d+(N/2)+1\right)|}_{\Delta^{\mathrm{MoD},d}(1)}$$
$$\times \underbrace{|r(d+2)-r\left(d+(N/2)+2\right)|}_{\Delta^{\mathrm{MoD},d}(2)},$$
$$\underbrace{|r(d+1)-r\left(d+(N/2)+1\right)|}_{\Delta^{\mathrm{MoD},d}(1)}$$
$$\times \underbrace{|r(d+3)-r\left(d+(N/2)+3\right)|}_{\Delta^{\mathrm{MoD},d}(3)},$$

$$\cdots,$$

$$\underbrace{|r(d+1)-r\left(d+(N/2)+1\right)|}_{\Delta^{\mathrm{MoD},d}(1)}$$
$$\times \underbrace{|r\left(d+(N/2)-1\right)-r(d+N-1)|}_{\Delta^{\mathrm{MoD},d}((N/2)-1)},$$

$$\cdots,$$

$$\left.\begin{aligned}&\underbrace{|r\left(d+(N/2)-2\right)-r(d+N-2)|}_{\Delta^{\mathrm{MoD},d}((N/2)-2)}\\ &\times \underbrace{|r\left(d+(N/2)-1\right)-r(d+N-1)|}_{\Delta^{\mathrm{MoD},d}((N/2)-1)}\end{aligned}\right\}. \quad (12)$$

The new normalization function utilizing the kth element of $\mathbf{Q}^{\mathrm{DDN},d}$, i.e., $Q^{\mathrm{DDN},d}(k)$, can be expressed as

$$R^{\mathrm{DDN}}(d)=\sum_{k=0}^{L-1}\left(Q^{\mathrm{DDN},d}(k)\right)^2 \quad (13)$$

where $L \le (N/4)((N/2)-1)$ is the correlation length, which is selected based on the desired performance of the metric (the longer the correlation length, the better the performance).

At the correct timing points $d=d_{\mathrm{pr}}$, without loss of generality, we consider $Q^{\mathrm{DDN},d}(0)$, and by replacing (2), we have

$$\begin{aligned}&\left(Q^{\mathrm{DDN},d_{\mathrm{pr}}}(0)\right)^2\\ &\quad=|r(d_{\mathrm{pr}})-r\left(d_{\mathrm{pr}}+(N/2)\right)|^2\\ &\qquad\times|r(d_{\mathrm{pr}}+1)-r\left(d_{\mathrm{pr}}+(N/2)+1\right)|^2\\ &\quad=\Big|y(d_{\mathrm{pr}})e^{j\frac{2\pi d_{\mathrm{pr}}}{N}\varepsilon}(1-e^{j\pi\varepsilon})\\ &\qquad+w(d_{\mathrm{pr}})-w\left(d_{\mathrm{pr}}+(N/2)\right)\Big|^2\\ &\qquad\times\Big|y(d_{\mathrm{pr}}+1)e^{j\frac{2\pi(d_{\mathrm{pr}}+1)}{N}\varepsilon}(1-e^{j\pi\varepsilon})\\ &\qquad+w(d_{\mathrm{pr}}+1)-w(d_{\mathrm{pr}}+(N/2)+1)\Big|^2 \quad (14)\end{aligned}$$

and consequently

$$\begin{aligned}E\left\{R^{\mathrm{DDN}}(d_{\mathrm{pr}})\right\}&=\sum_{k=0}^{L-1}E\left\{\left(Q^{\mathrm{DDN},d_{\mathrm{pr}}}(k)\right)^2\right\}\\ &=LE\left\{\left(Q^{\mathrm{DDN},d_{\mathrm{pr}}}(0)\right)^2\right\}\\ &=L\left(\sigma_y^2\left|1-e^{j\pi\varepsilon}\right|^2+2\sigma_w^2\right)^2 \quad (15)\end{aligned}$$

where $\sigma_y^2=E\{|y(k)|^2\}$.

At the wrong timing points $d=d_{\mathrm{ab}}$, we have

$$\begin{aligned}&\left(Q^{\mathrm{DDN},d_{\mathrm{ab}}}(0)\right)^2\\ &\quad=|r(d_{\mathrm{ab}})-r\left(d_{\mathrm{ab}}+(N/2)\right)|^2\\ &\qquad\times|r(d_{\mathrm{ab}}+1)-r\left(d_{\mathrm{ab}}+(N/2)+1\right)|^2\\ &\quad=|w(d_{\mathrm{ab}})-w\left(d_{\mathrm{ab}}+(N/2)\right)|^2\\ &\qquad\times|w(d_{\mathrm{ab}}+1)-w\left(d_{\mathrm{ab}}+(N/2)+1\right)|^2 \quad (16)\end{aligned}$$

and consequently

$$\begin{aligned}E\left\{R^{\mathrm{DDN}}(d_{\mathrm{ab}})\right\}&=\sum_{k=0}^{L-1}E\left\{\left(Q^{\mathrm{DDN},d_{\mathrm{ab}}}(k)\right)^2\right\}\\ &=LE\left\{\left(Q^{\mathrm{DDN},d_{\mathrm{ab}}}(0)\right)^2\right\}=4L\sigma_w^4. \quad (17)\end{aligned}$$

Knowing from [10] that

$$E\left\{|P(d)|\right\}=\begin{cases}L\sigma_y^4, & d=d_{\mathrm{pr}}\\ \frac{\sqrt{\pi L}}{2}\sigma_w^4, & d=d_{\mathrm{ab}}\end{cases} \quad (18)$$

and by applying the normalization values in (15) and (17), the expected values of the proposed timing metric $E\{T^{\mathrm{DDN}}(d)\}=E\{|P(d)|/R^{\mathrm{DDN}}(d)\}$, at the correct timing points d_{pr} and wrong timing points d_{ab}, become

$$\begin{aligned}E\left\{T^{\mathrm{DDN}}(d)\right\}&=E\left\{\frac{|P(d)|}{R^{\mathrm{DDN}}(d)}\right\}\approx\frac{E\left\{|P(d)|\right\}}{E\left\{R^{\mathrm{DDN}}(d)\right\}}\\ &=\begin{cases}\frac{1}{\left(|1-e^{j\pi\varepsilon}|^2+\frac{2}{SNR}\right)^2}, & d=d_{\mathrm{pr}}\\ \frac{1}{8}\sqrt{\frac{\pi}{L}}, & d=d_{\mathrm{ab}}\end{cases} \quad (19)\end{aligned}$$

where $\mathrm{SNR}=\sigma_y^2/\sigma_w^2$. In the given equation, we have used the approximation $E\{|P(d)|/R^{\mathrm{DDN}}(d)\}\approx E\{|P(d)|\}/E\{R^{\mathrm{DDN}}(d)\}$, which is obtained from the Taylor series expansion of $E\{|P(d)|/R^{\mathrm{DDN}}(d)\}$ about the means $E\{|P(d)|\}$ and $E\{R^{\mathrm{DDN}}(d)\}$ [22]. We have chosen the first-order term and ignored the higher order terms because of the laborious calculations. The simulation results provided in Figs. 3–7 also confirm the accuracy of the approximation.

Assuming that CFO (ε) is negligible, $E\{T^{\mathrm{DDN}}(d)\}$ can be approximated as

$$E\left\{T^{\mathrm{DDN}}(d)\right\} \approx \begin{cases} \frac{SNR^2}{4}, & d = d_{\mathrm{pr}} \\ \frac{1}{8}\sqrt{\frac{\pi}{L}}, & d = d_{\mathrm{ab}}. \end{cases} \tag{20}$$

From the comparison of (20) and $E\{T_{Z,\mathrm{MoD}}(d_{\mathrm{pr}})\} \approx \mathrm{SNR}/2$ in [9], it is concluded that since we have $E\{T^{\mathrm{DDN}}(d_{\mathrm{pr}})\} > E\{T_{Z,\mathrm{MoD}}(d_{\mathrm{pr}})\}$ for SNR > 3 dB, the new method has a greater peak at the correct timing instants for SNR $>$ 3 dB (further comparisons will be discussed in the following section).

For the devices that are compatible with some standards, the tolerable range of CFO is generally available and specified in the standard. Under the circumstances that CFO is small (such as in IEEE802.11n WLAN), the proposed normalization function in (13) can be applied [9]. For other cases, we propose to adopt the following approach for normalization of the timing metric.

B. CFO-Independent DDN (CIDDN)

To design a normalization function that is not affected by the CFO, we directly use the absolute value of the received signal in the normalization function. This approach can be clarified by considering the DoM normalization scheme in [9], which obtains the energy of the following vector:

$$\Delta^{\mathrm{DoM},d} = \Bigg\{ \underbrace{|r(d)| - |r\left(d + (N/2)\right)|}_{\Delta^{\mathrm{DoM},d}(0)}, \underbrace{|r(d+1)| - |r\left(d + (N/2) + 1\right)|}_{\Delta^{\mathrm{DoM},d}(1)}, \ldots, \underbrace{|r\left(d + (N/2) - 1\right)| - |r(d + N - 1)|}_{\Delta^{\mathrm{DoM},d}((N/2)-1)} \Bigg\}. \tag{21}$$

For the new normalization function, we propose to use the products of the elements of $\Delta^{\mathrm{DoM},d}$ in the following way:

$$\begin{aligned} \mathbf{Q}^{\mathrm{CIDDN},d} = \Bigg\{ & \underbrace{\left(|r(d)| - |r\left(d + (N/2)\right)|\right)}_{\Delta^{\mathrm{DoM},d}(0)} \times \underbrace{\left(|r(d+1)| - |r\left(d + (N/2) + 1\right)|\right)}_{\Delta^{\mathrm{DoM},d}(1)}, \\ & \underbrace{\left(|r(d)| - |r\left(d + (N/2)\right)|\right)}_{\Delta^{\mathrm{DoM},d}(0)} \times \underbrace{\left(|r(d+2)| - |r\left(d + (N/2) + 2\right)|\right)}_{\Delta^{\mathrm{DoM},d}(2)}, \\ & \ldots, \\ & \underbrace{\left(|r(d)| - |r\left(d + (N/2)\right)|\right)}_{\Delta^{\mathrm{DoM},d}(0)} \times \underbrace{\left(|r\left(d + (N/2) - 1\right)| - |r(d + N - 1)|\right)}_{\Delta^{\mathrm{DoM},d}((N/2)-1)}, \\ & \underbrace{\left(|r(d+1)| - |r\left(d + (N/2) + 1\right)|\right)}_{\Delta^{\mathrm{DoM},d}(1)} \times \underbrace{\left(|r(d+1)| - |r\left(d + (N/2) + 1\right)|\right)}_{\Delta^{\mathrm{DoM},d}(1)}, \\ & \underbrace{\left(|r(d+2)| - |r\left(d + (N/2) + 2\right)|\right)}_{\Delta^{\mathrm{DoM},d}(2)} \times \underbrace{\left(|r(d+1)| - |r\left(d + (N/2) + 1\right)|\right)}_{\Delta^{\mathrm{DoM},d}(1)}, \\ & \underbrace{\left(|r(d+3)| - |r\left(d + (N/2) + 3\right)|\right)}_{\Delta^{\mathrm{DoM},d}(3)} \times \ldots, \\ & \underbrace{\left(|r(d+1)| - |r\left(d + (N/2) + 1\right)|\right)}_{\Delta^{\mathrm{DoM},d}(1)} \times \underbrace{\left(|r\left(d + (N/2) - 1\right)| - |r(d + N - 1)|\right)}_{\Delta^{\mathrm{DoM},d}((N/2)-1)}, \\ & \ldots, \\ & \underbrace{\left(|r\left(d + (N/2) - 2\right)| - |r\left(d + N - 2\right)|\right)}_{\Delta^{\mathrm{DoM},d}((N/2)-2)} \times \underbrace{\left(|r\left(d + (N/2) - 1\right)| - |r(d + N - 1)|\right)}_{\Delta^{\mathrm{DoM},d}((N/2)-1)} \Bigg\} \end{aligned} \tag{22}$$

and take advantage of the elements of $\mathbf{Q}^{\mathrm{CIDDN},d}$, i.e., $Q^{\mathrm{CIDDN},d}(k)$. Therefore, the normalization function is proposed as

$$R^{\mathrm{CIDDN}}(d) = \sum_{k=0}^{L-1} \left(Q^{\mathrm{CIDDN},d}(k)\right)^2. \tag{23}$$

The mean values of the normalization function at the correct and wrong timing points is derived in the Appendix and can be expressed as

$$E\left\{R^{\mathrm{CIDDN}}(d)\right\} = \begin{cases} \leq 4L\sigma_w^4, & d = d_{\mathrm{pr}} \\ \left(2 - \frac{\pi}{2}\right)^2 L\sigma_w^4, & d = d_{\mathrm{ab}}. \end{cases} \tag{24}$$

Considering (18) and (24) and using the same approximations applied to (19), the new timing metric $T^{\mathrm{CIDDN}}(d) = |P(d)|/R^{\mathrm{CIDDN}}(d)$ has the following mean values:

$$\begin{aligned} E\left\{T^{\mathrm{CIDDN}}(d)\right\} &= E\left\{\frac{|P(d)|}{R^{\mathrm{CIDDN}}(d)}\right\} \approx \frac{E\left\{|P(d)|\right\}}{E\left\{R^{\mathrm{CIDDN}}(d)\right\}} \\ &= \begin{cases} \geq \frac{\sigma_y^4}{4\sigma_w^4} = \frac{\mathrm{SNR}^2}{4}, & d = d_{\mathrm{pr}} \\ \frac{1}{2\left(2-\frac{\pi}{2}\right)^2}\sqrt{\frac{\pi}{L}}, & d = d_{\mathrm{ab}}. \end{cases} \end{aligned} \tag{25}$$

It is observed that the mean value of the proposed normalization function $E\{R^{\mathrm{CIDDN}}(d)\}$ and, consequently, the mean value of the timing metric $E\{T^{\mathrm{CIDDN}}(d)\}$ are not affected by the CFO.

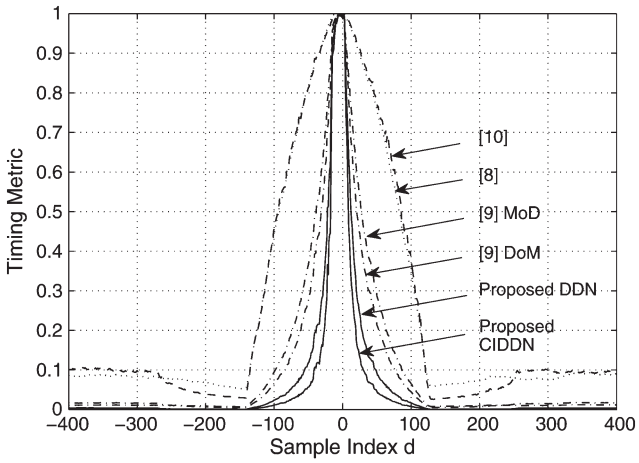

Fig. 1. Proposed timing metrics in comparison with previous methods averaged over 100 realizations in the SUI-1 channel ($N = 256$ and $N_g = 16$).

To give further explanation to why the new timing metric is not affected by the CFO, without loss of generality, we consider the received signal $r(d)$. We have

$$\begin{aligned} |r(d)| &= \left| y(d)e^{j\frac{2\pi d}{N}\varepsilon} + w(d) \right| \\ &= \left| e^{j\frac{2\pi d}{N}\varepsilon} \left(y(d) + e^{-j\frac{2\pi d}{N}\varepsilon} w(d) \right) \right| \\ &= \left| e^{j\frac{2\pi d}{N}\varepsilon} \right| \left| y(d) + e^{-j\frac{2\pi d}{N}\varepsilon} w(d) \right| \\ &= \left| y(d) + e^{-j\frac{2\pi d}{N}\varepsilon} w(d) \right| = |y(d) + w(d)|. \end{aligned} \quad (26)$$

In the given equation, multiplying $e^{-j(2\pi d/N)\varepsilon}$ and $w(d)$ does not change the mean and variance of the noise term; therefore, $e^{-j(2\pi d/N)\varepsilon} w(d)$ is still a noise sample with the same mean and variance as $w(d)$; hence, we can replace $e^{-j(2\pi d/N)\varepsilon} w(d)$ with $w(d)$ in (26). It is obvious in (26) that by taking the absolute value of $r(d)$, the effect of CFO is removed from the received signal. Therefore, the elements $Q^{\mathrm{CIDDN},d}(k)$ in (22) (for example, $Q^{\mathrm{CIDDN},d}(0) = (|r(d)| - |r(d + (N/2))|)(|r(d+1)| - |r(d + (N/2) + 1)|)$) are not affected by the CFO. Consequently, the normalization function in (23), i.e., $R^{\mathrm{CIDDN}}(d) = \sum_{k=0}^{L-1} \left(Q^{\mathrm{CIDDN},d}(k)\right)^2$, is also not affected by the CFO. Moreover, knowing from [10] that the absolute value of the correlation function $|P(d)|$ is not changed by the CFO, it is concluded that the proposed timing metric $T^{\mathrm{CIDDN}}(d) = |P(d)|/R^{\mathrm{CIDDN}}(d)$ is independent of the CFO.

In Fig. 1, we have shown the proposed timing metrics along with the previous metrics, where all of them are normalized to their maximum values. It is evident that our proposed timing metrics, due to the use of the fourth-order normalization, have considerably sharper peaks. In this figure, the CFO for MoD [9] and the proposed DDN method is set to $\varepsilon = 0.1$, and for [8], [10], DoM [9], and the proposed CIDDN, it is set to $\varepsilon = 4.3$.

IV. Theoretical Performance Evaluation

To evaluate the performance theoretically and show that, at the correct and incorrect timing points, the new metrics have values that are more distinct in comparison with the previous methods, we make use of two criteria. The first criterion is that used in [9] and applies the mean values of timing metrics. The second criterion takes advantage of both mean and variance for comparing different metrics. Furthermore, the computational complexity of the proposed methods are compared with the previous schemes.

A. Mean of Timing Metrics as the Criterion for Between-Class Distance

Here, we apply the same performance evaluation criterion as in [9]. Therefore, we choose the difference between the mean values of the new metrics at the correct and wrong timing points as the criterion for performance evaluation. This criterion in classification theory is a measure of between-class distance assessment for different classifiers and is referred to as the class-separability criterion [19] (It is worth mentioning that the performance can also be assessed in terms of false alarm and missed detection probabilities. Since the theoretical derivation of false alarm and missed detection probabilities can involve too many approximations, these probabilities are obtained by simulation in Section V).

Similar to [9], we use the following factor for class-separability comparisons:

$$\alpha^{\mathrm{new}}_{\mathrm{conventional}} = \frac{E\left\{T^{\mathrm{new}}(d_{\mathrm{pr}})\right\} / E\left\{T^{\mathrm{new}}(d_{\mathrm{ab}})\right\}}{E\left\{T_{\mathrm{conventional}}(d_{\mathrm{pr}})\right\} / E\left\{T_{\mathrm{conventional}}(d_{\mathrm{ab}})\right\}} \quad (27)$$

where $\alpha^{\mathrm{new}}_{\mathrm{conventional}}$ is used to compare the new timing metric with the conventional metrics. By $T^{\mathrm{new}}(d)$, we mean either $T^{\mathrm{DDN}}(d)$ in (19) or $T^{\mathrm{CIDDN}}(d)$ in (25), and $T_{\mathrm{conventional}}(d)$ denotes the proposed metrics in [8], [9], or [10].

The factor $\alpha^{\mathrm{new}}_{\mathrm{conventional}}$ indicates that between the two timing metrics ($T^{\mathrm{new}}(d)$ and $T_{\mathrm{conventional}}(d)$), the timing metric whose difference value between the correct and wrong timing points is greater has better performance. Therefore, when $\alpha^{\mathrm{new}}_{\mathrm{conventional}} > 1$, our metric achieves better performance than $T_{\mathrm{conventional}}(d)$. Now, using this criterion, we compare the proposed methods with the previous methods.

1) Comparison of the Proposed Methods With the Method in [8]: When $T_{\mathrm{conventional}}(d) = T_R(d)$, where $T_R(d)$ is the metric proposed in [8] with the mean values

$$E\left\{T_R(d)\right\} = \begin{cases} \frac{1}{1+\frac{1}{\mathrm{SNR}}}, & d = d_{\mathrm{pr}} \\ \sqrt{\frac{\pi}{2N}}, & d = d_{\mathrm{ab}} \end{cases} \quad (28)$$

and $T^{\mathrm{new}}(d) = T^{\mathrm{DDN}}(d)$ [considering(19)], the factor α_R^{DDN} becomes

$$\begin{aligned} \alpha_R^{\mathrm{DDN}} &= \frac{\frac{1}{\left(|1-e^{j\pi\varepsilon}|^2 + \frac{2}{SNR}\right)^2}}{\frac{1}{\left(1+\frac{1}{SNR}\right)}} \frac{\sqrt{\frac{\pi}{2N}}}{\frac{1}{8}\sqrt{\frac{\pi}{L}}} \\ &= \frac{8\left(1+\frac{1}{SNR}\right)}{\left(|1-e^{j\pi\varepsilon}|^2 + \frac{2}{SNR}\right)^2} \sqrt{\frac{L}{2N}} \end{aligned} \quad (29)$$

which, for small values of CFO, can be simplified as

$$\alpha_R^{\mathrm{DDN}} = (\mathrm{SNR}^2 + \mathrm{SNR})\sqrt{\frac{2L}{N}}. \tag{30}$$

According to (30), for SNR ≥ 0 dB and $L \geq (N/2)$, we have $\alpha_R^{\mathrm{DDN}} > 1$. This means that our method achieves better performance in comparison with that in [8] even for low SNRs and low correlation lengths, provided that the CFO is negligible.

To compare the class separability of the second proposed method $T^{\mathrm{CIDDN}}(d)$ with that in [8], we consider (25) and (28), and the lower bound for the factor $\alpha_R^{\mathrm{CIDDN}}$ is obtained as

$$\alpha_R^{\mathrm{CIDDN}} \geq \frac{\frac{\mathrm{SNR}^2}{4}}{\frac{1}{\left(1+\frac{1}{\mathrm{SNR}}\right)}} \frac{\sqrt{\frac{\pi}{2N}}}{\frac{1}{2\left(2-\frac{\pi}{2}\right)^2}\sqrt{\frac{\pi}{L}}}$$

$$= \frac{1}{2}\left(2-\frac{\pi}{2}\right)^2 (\mathrm{SNR}^2 + \mathrm{SNR})\sqrt{\frac{L}{2N}}. \tag{31}$$

It is observed that for $L \geq 2N$ and SNR ≥ 5 dB, we have $\alpha_R^{\mathrm{CIDDN}} > 1$, and our second method, which is robust to CFO, has better performance than that in [8]. It is worth noting that (31) is the lower bound, and the performance can be better than what is indicated by (31), as will be shown in Section V.

2) Comparison of the Proposed Methods With the Methods in [9]: If $T_{\mathrm{conventional}}(d) = T_{Z,\mathrm{MoD}}(d)$, where $T_{Z,\mathrm{MoD}}(d)$ is the MoD metric proposed in [9] with the mean values

$$E\left\{T_{Z,\,\mathrm{MoD}}(d)\right\} = \begin{cases} \frac{1}{|1-e^{j\pi\varepsilon}|^2+\frac{2}{SNR}}, & d = d_{\mathrm{pr}} \\ \sqrt{\frac{\pi}{8N}}, & d = d_{\mathrm{ab}} \end{cases} \tag{32}$$

then considering (19), we have

$$\alpha_{Z,\,\mathrm{MoD}}^{\mathrm{DDN}} = \frac{\frac{1}{\left(|1-e^{j\pi\varepsilon}|^2+\frac{2}{\mathrm{SNR}}\right)^2}}{\frac{1}{|1-e^{j\pi\varepsilon}|^2+\frac{2}{SNR}}} \frac{\sqrt{\frac{\pi}{8N}}}{\frac{1}{8}\sqrt{\frac{\pi}{L}}} = \frac{2\sqrt{2}}{|1-e^{j\pi\varepsilon}|^2+\frac{2}{\mathrm{SNR}}}\sqrt{\frac{L}{N}}. \tag{33}$$

For small values of CFO, (33) is approximated as

$$\alpha_{Z,\,\mathrm{MoD}}^{\mathrm{DDN}} = \mathrm{SNR}\sqrt{\frac{2L}{N}}. \tag{34}$$

According to this equation, for SNR > 0 dB and $L \geq N/2$, we have $\alpha_{Z,\mathrm{MoD}}^{\mathrm{DDN}} > 1$. Therefore, when the CFO is negligible, even for small values of the correlation length and SNR, our method improves the performance. Moreover, the increase in SNR and correlation length significantly enhances the performance.

It is notable that since only a lower bound is obtained for both the DoM metric in [9] and for $T^{\mathrm{CIDDN}}(d)$ at the correct timing points in (25), it is not possible to theoretically derive the factor $\alpha_{Z,\mathrm{DoM}}^{\mathrm{CIDDN}}$. In Section V, to compare $T^{\mathrm{CIDDN}}(d)$ with the DoM timing metric in [9], we obtain $\alpha_{Z,\mathrm{DoM}}^{\mathrm{CIDDN}}$ by simulation, which confirms that the new method has a remarkably better performance.

3) Comparison of the Proposed Methods With the Method in [10]: When $T_{\mathrm{conventional}}(d) = T_A(d)$, where $T_A(d)$ is the metric proposed in [10] with the mean values

$$E\left\{T_A(d)\right\} = \begin{cases} \frac{1}{\left(1+\frac{2}{\mathrm{SNR}}+\frac{1}{\mathrm{SNR}^2}\right)}, & d = d_{\mathrm{pr}} \\ \sqrt{\frac{\pi}{4L}}, & d = d_{\mathrm{ab}} \end{cases} \tag{35}$$

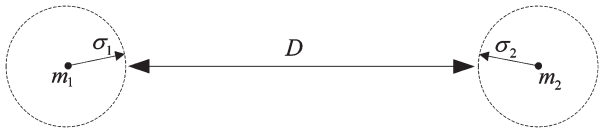

Fig. 2. Between-class distance $D = |(m_2 - \sigma_2) - (m_1 + \sigma_1)|$, using both the mean and variance of the timing metrics knowing that $m_2 > m_1$ and $m_2 - m_1 > \sigma_1 + \sigma_2$.

the factor α_A^{DDN} becomes

$$\alpha_A^{\mathrm{DDN}} = \frac{\frac{1}{\left(|1-e^{j\pi\varepsilon}|^2+\frac{2}{SNR}\right)^2}}{\frac{1}{\left(1+\frac{2}{SNR}+\frac{1}{SNR^2}\right)}} \frac{\sqrt{\frac{\pi}{4L}}}{\frac{1}{8}\sqrt{\frac{\pi}{L}}} = \frac{4\left(1+\frac{2}{SNR}+\frac{1}{SNR^2}\right)}{\left(|1-e^{j\pi\varepsilon}|^2+\frac{2}{SNR}\right)^2}. \tag{36}$$

The small values of CFO results in

$$\alpha_A^{\mathrm{DDN}} = \mathrm{SNR}^2 + 2\mathrm{SNR} + 1 \tag{37}$$

which demonstrates that for SNR > 0 dB, we have $\alpha_A^{\mathrm{DDN}} > 1$, and factor α_A^{DDN} is independent of the correlation length.

For the case $T^{\mathrm{new}}(d) = T^{\mathrm{CIDDN}}(d)$, the lower bound for factor $\alpha_A^{\mathrm{CIDDN}}$ becomes

$$\alpha_A^{\mathrm{CIDDN}} \geq \frac{\frac{SNR^2}{4}}{\frac{1}{\left(1+\frac{2}{SNR}+\frac{1}{SNR^2}\right)}} \frac{\sqrt{\frac{\pi}{4L}}}{\frac{1}{2\left(2-\frac{\pi}{2}\right)^2}\sqrt{\frac{\pi}{L}}}$$

$$= \frac{1}{4}\left(2-\frac{\pi}{2}\right)^2 (\mathrm{SNR}^2 + 2\,\mathrm{SNR} + 1). \tag{38}$$

Therefore, for SNR > 6 dB, we have $\alpha_A^{\mathrm{CIDDN}} > 1$.

B. Mean and Variance of Timing Metrics as the Criterion for Between-Class Distance

To evaluate class separability, using both the means and variances of the timing metrics, we define the distance between the two classes (as shown in Fig. 2) in the following way:

$$D = |(m_2 - \sigma_2) - (m_1 + \sigma_1)| \tag{39}$$

where m_1 and σ_1 represent the mean and standard deviation of the metric at the wrong timing points. In the same way, m_2 and σ_2 indicate the mean and standard deviation of the metric at the correct timing points. Note that in defining D in (39), we have considered the fact that under normal conditions (for example, in practical SNRs or for $N \geq 32$) for the timing metrics, we have $m_2 > m_1$ and $m_2 - m_1 > \sigma_1 + \sigma_2$ (which can be easily checked).

For the metric proposed in [8], we have $m_1 = \sqrt{\pi/(2N)}$, $\sigma_1^2 = (2-(\pi/2))(1/N)$, and $m_2 = 1/(1+(1/\mathrm{SNR}))$. As obtained in [10], we have the following values for the metric in [10]: $m_1 \approx \sqrt{(\pi/2)(1/(2L))}$, $\sigma_1^2 = (2-(\pi/2))(1/(2L))$, and $m_2 \approx 1/[1 + (2/\mathrm{SNR}) + (1/\mathrm{SNR})^2]$. Furthermore, we have the values $m_1 = \sqrt{\pi/(8N)}$, $\sigma_1^2 = (1/(2N))(1 - (\pi/4))$, and $m_2 = 1/[|1 - e^{j\pi\varepsilon}|^2 + (2/\mathrm{SNR})]$ for the MoD metric in [9]. For the DDN method, according to (19), we have $m_1 = (1/8)\sqrt{\pi/L}$, $\sigma_1^2 = (2-(\pi/2))(1/(32L))$, and $m_2 = 1/(|1-e^{j\pi\varepsilon}|^2+(2/\mathrm{SNR}))^2$. Since calculating σ_2^2 theoretically for all four cases is an arduous task, we have made use of computer simulation for

obtaining σ_2^2. Moreover, due to having a lower bound for the DoM [9] and CIDDN, we have utilized simulation for showing D for these methods.

In Section V (see Figs. 7–9), using the given criterion, we have demonstrated the performance of the new methods along with those of previous methods. The comparison reveals the outstanding performance of the proposed methods.

C. Computational Complexity

To calculate the complexity of the new normalization methods, we first rewrite the elements of $\mathbf{Q}^{\mathrm{DDN},d}$ in (12) in the new equivalent form as

$$\mathbf{Q}^{\mathrm{DDN},d} = \left\{ Q_1^{\mathrm{DDN},d}, Q_2^{\mathrm{DDN},d}, \ldots, Q_{(N/2)-1}^{\mathrm{DDN},d} \right\} \tag{40}$$

where $Q_n^{\mathrm{DDN},d}$ is the nth subvector of $\mathbf{Q}^{\mathrm{DDN},d}$, which is defined as

$$\begin{aligned} Q_n^{\mathrm{DDN},d} = \{ & |r(d) - r(d+(N/2))|, \\ & |r(d+1) - r(d+(N/2)+1)|, \\ & \cdots, \\ & |r(d+(N/2)-n-1) - r(d+N-n-1)|\} \\ \circ \{ & |r(d+n) - r(d+n+(N/2))|, \\ & |r(d+n+1) - r(d+n+(N/2)+1)|, \\ & \cdots, \\ & |r(d+(N/2)-1) - r(d+N-1)|\}. \end{aligned} \tag{41}$$

In the given equation, the operator $\circ$ is the Hadamard product and denotes element-by-element multiplication of the two vectors.

If, for simplicity and without loss of generality, we assume that $\mathbf{Q}^{\mathrm{DDN},d}$ has only its first subvector, i.e., $\mathbf{Q}^{\mathrm{DDN},d} = \{Q_1^{\mathrm{DDN},d}\}$; then, at time instants d and $d+1$, we, respectively, have

$$\begin{aligned} & \mathbf{Q}^{\mathrm{DDN},d} \\ & = \{ |r(d) - r(d+(N/2))|\, |r(d+1) - r(d+(N/2)+1)|, \\ & \quad |r(d+1) - r(d+(N/2)+1)| \\ & \quad \times |r(d+2) - r(d+(N/2)+2)|, \ldots, \\ & \quad |r(d+(N/2)-2) - r(d+N-2)| \\ & \quad \times |r(d+(N/2)-1) - r(d+N-1)|\} \end{aligned} \tag{42}$$

$$\begin{aligned} & \mathbf{Q}^{\mathrm{DDN},d+1} \\ & = \{ |r(d+1) - r(d+(N/2)+1)| \\ & \quad \times |r(d+2) - r(d+(N/2)+2)|, \\ & \quad |r(d+2) - r(d+(N/2)+2)| \\ & \quad \times |r(d+3) - r(d+(N/2)+3)|, \ldots, \\ & \quad |r(d+(N/2)-1) - r(d+N-1)| \\ & \quad \times |r(d+(N/2)) - r(d+N)|\}. \end{aligned} \tag{43}$$

TABLE I
COMPUTATIONAL COMPLEXITY OF NORMALIZATION METHODS

Method	Real Multiplications	Real Additions
[2], [8]	-	3
[9] MoD	-	7
[9] DoM	-	5
[10]	$16N_s$, $1 \le N_s \le (N/2)-1$	$13N_s$, $1 \le N_s \le (N/2)-1$
Proposed DDN	$2N_s$, $1 \le N_s \le (N/2)-1$	$10N_s$, $1 \le N_s \le (N/2)-1$
Proposed CIDDN	$2N_s$, $1 \le N_s \le (N/2)-1$	$6N_s$, $1 \le N_s \le (N/2)-1$

It is observed that we can write the elements of $\mathbf{Q}^{\mathrm{DDN},d+1}$ in terms of the elements of $\mathbf{Q}^{\mathrm{DDN},d}$ as follows:

$$\begin{aligned} & \mathbf{Q}^{\mathrm{DDN},d+1} \\ & = \{ Q^{\mathrm{DDN},d}(1), Q^{\mathrm{DDN},d}(2), \ldots, Q^{\mathrm{DDN},d}((N/2)\text{–}2), \\ & \quad |r(d+(N/2)-1) - r(d+N-1)| \\ & \quad \times |r(d+(N/2)) - r(d+N)|\}. \end{aligned} \tag{44}$$

Thus, for $R^{\mathrm{DDN}}(d)$, we have

$$\begin{aligned} & R^{\mathrm{DDN}}(d+1) \\ & = R^{\mathrm{DDN}}(d) - (|r(d) - r(d+(N/2))| \\ & \qquad \times |r(d+1) - r(d+(N/2)+1)|)^2 \\ & \quad + (|r(d+(N/2)-1) - r(d+N-1)| \\ & \qquad \times |r(d+(N/2)) - r(d+N)|)^2. \end{aligned} \tag{45}$$

Therefore, the proposed normalization function needs two real multiplications, four complex additions, and two real additions for each subvector of $\mathbf{Q}^{\mathrm{DDN},d}$ at each timing instant d. Consequently, for the $N_s (1 \le N_s \le (N/2)-1)$ subvectors of $\mathbf{Q}^{\mathrm{DDN},d}$, we need $2N_s$ real multiplications, $4N_s$ complex additions, and $2N_s$ real additions at each timing instant d.

Adopting the same approach, it is straightforward to show that the second proposed normalization function $R^{\mathrm{CIDDN}}(d)$ can be written in the following form:

$$\begin{aligned} R^{\mathrm{CIDDN}}(d+1) = & R^{\mathrm{CIDDN}}(d) - (|r(d)| - |r(d+(N/2))|)^2 \\ & \times (|r(d+1)| - |r(d+(N/2)+1)|)^2 \\ & + (|r(d+(N/2)-1)| - |r(d+N-1)|)^2 \\ & \times (|r(d+(N/2))| - |r(d+N)|)^2 \end{aligned} \tag{46}$$

and therefore, $2N_s (1 \le N_s \le (N/2)-1)$ real multiplications and $6N_s$ real additions at each timing instant d need to be computed.

In Table I, we have shown the computational complexity of different normalization methods considering that each complex additions is tantamount to two real additions, and each complex multiplication is equivalent to four real multiplications and two real additions. According to this table, the new method has higher complexity than those in [2], [8], and [9] but has

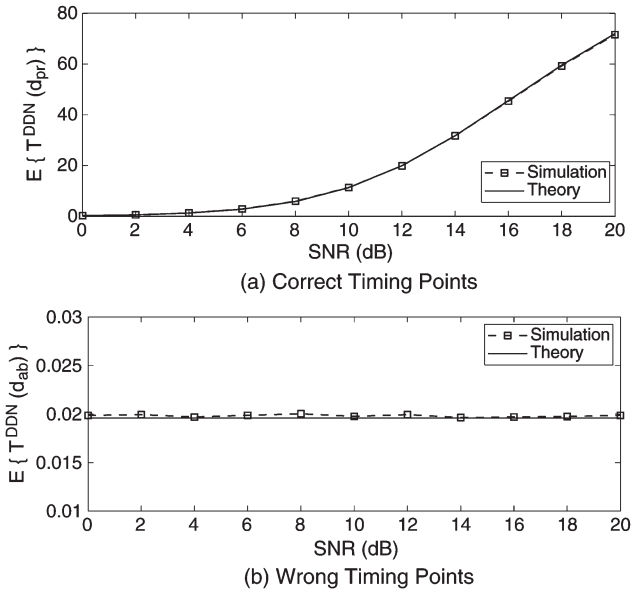

Fig. 3. Comparisons between the mean values of the proposed timing metric derived in (19) and the mean values obtained by simulations in the SUI-1 channel for different SNRs ($N = 256$, $L = N/2$, and $N_g = 16$). (a) Correct timing points ($d = d_{\rm pr}$). (b) Wrong timing points ($d = d_{\rm ab}$).

significantly lower complexity than that in [10]. It is notable that the new methods, even for small values of N_s, significantly improve the performance (for example, for $N_s = 1$, which results in the correlation length $L \approx N/2$, they need two real multiplications).

V. Results

Computer simulations have been run to evaluate the performance of the proposed methods in comparison with the previous methods and to verify the theoretical results. The parameters used in the simulations of the OFDM system are as follows: the number of the subcarriers is 256, the CP length is 16, the sampling rate is 10 MHz, and the multipath fading channel is Stanford University Interim (SUI) channel modeling, i.e., SUI-1 [21]. In the figures illustrated here, wherever there is a curve corresponding to the proposed DDN method or MoD method [9], the normalized CFO is chosen $\varepsilon = 0.1$; otherwise, the normalized CFO is set to $\varepsilon = 4.3$.

In Fig. 3(a) and (b), we have compared the theoretical mean values of the proposed timing metric described by (19) with the corresponding mean values obtained by simulation in the correct and wrong timing points, respectively. These figures are illustrated for different values of SNRs and $L = N/2$. It can be seen that the simulation results verify the accuracy of approximation applied to (19).

In Fig. 4, we have shown the factors $\alpha_R^{\rm DDN}$, $\alpha_{Z,{\rm MoD}}^{\rm DDN}$, and $\alpha_A^{\rm DDN}$ for different correlation lengths L and SNRs using theory and simulation. Considering $\alpha_R^{\rm DDN}$, our method achieves better performance compared with [8] ($\alpha_R^{\rm DDN} > 1$) and improves further with the increase in correlation length and SNR. Moreover, simulation results verify the theoretical derivation in (29). The next curves, i.e., $\alpha_{Z,{\rm MoD}}^{\rm DDN}$, indicate improved performance of the proposed method for SNR > 0 dB in comparison with [9] and

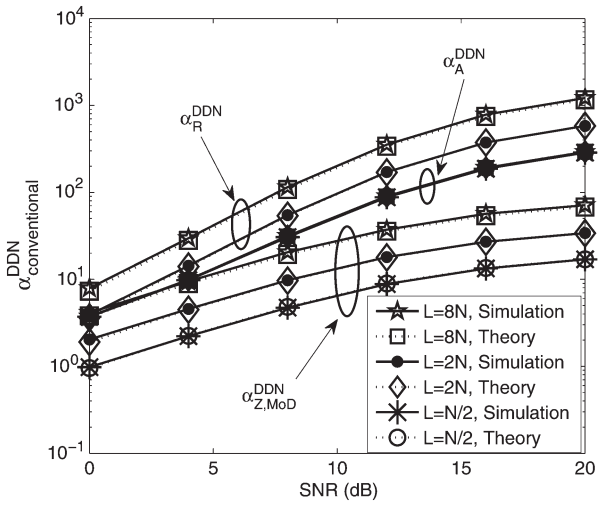

Fig. 4. Factors $\alpha_R^{\rm DDN}$, $\alpha_{Z,{\rm MoD}}^{\rm DDN}$, and $\alpha_A^{\rm DDN}$ comparing the class separability of the proposed method [$T^{\rm DDN}(d)$ in (19)] with those in [8]–[10], respectively, for different correlation lengths L and SNRs, obtained both theoretically and by simulations in the SUI-1 channel ($N = 256$ and $N_g = 16$).

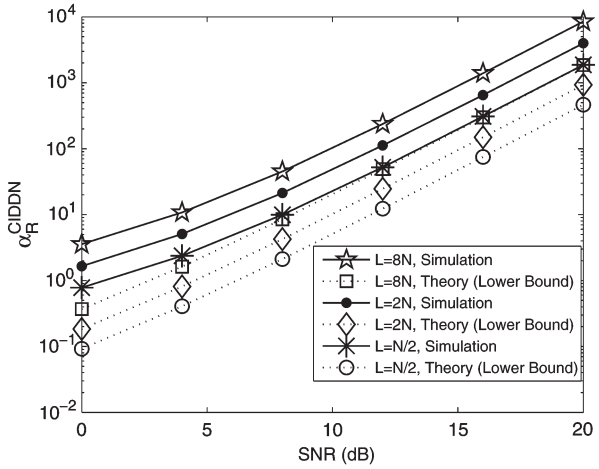

Fig. 5. Factor $\alpha_R^{\rm CIDDN}$ comparing the class separability of the proposed method [$T^{\rm CIDDN}(d)$ in (25)] with that in [8] for different correlation lengths L and SNRs, obtained both theoretically and by simulations in the SUI-1 channel ($N = 256$ and $N_g = 16$).

the factor $\alpha_A^{\rm DDN}$ compares the enhanced class separability of the proposed DDN metric with the metric presented in [10]. Due to being independent of the correlation length, $\alpha_A^{\rm DDN}$ has the same curve for different correlation lengths.

Fig. 5 shows the theoretical lower bound for $\alpha_R^{\rm CIDDN}$ in (31) and actual values of $\alpha_R^{\rm CIDDN}$ for different correlation lengths acquired from simulation. As expected, the simulation results have higher values than the theoretical lower bounds. Furthermore, for SNR > 1 dB and for all the correlation lengths, we have $\alpha_R^{\rm CIDDN} > 1$, which indicates that our method outperforms the method in [8].

The comparison between the proposed $T^{\rm CIDDN}(d)$ and the DoM timing metric in [9] is done by depicting $\alpha_{Z,{\rm DoM}}^{\rm CIDDN}$ obtained using simulation in Fig. 6. According to this figure, for $L \geq 2N$, we have a better performance ($\alpha_{Z,{\rm DoM}}^{\rm CIDDN} > 1$) for every SNR. The improvement in the performance can also be acquired using the correlation length $L = N/2$ and SNR $\geq$

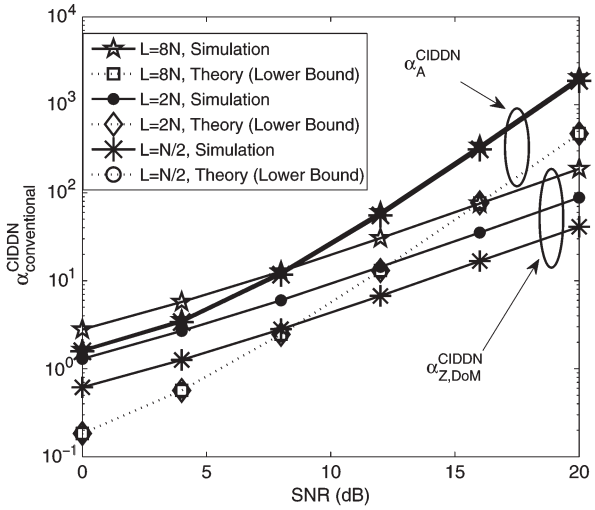

Fig. 6. Factors $\alpha_{Z,\mathrm{DoM}}^{\mathrm{CIDDN}}$ and $\alpha_A^{\mathrm{CIDDN}}$ comparing the class separability of the proposed method [$T^{\mathrm{CIDDN}}(d)$ in (25)] with those in [9] and [10], respectively, for different correlation lengths L and SNRs, obtained both theoretically and by simulations in the SUI-1 channel ($N = 256$ and $N_g = 16$).

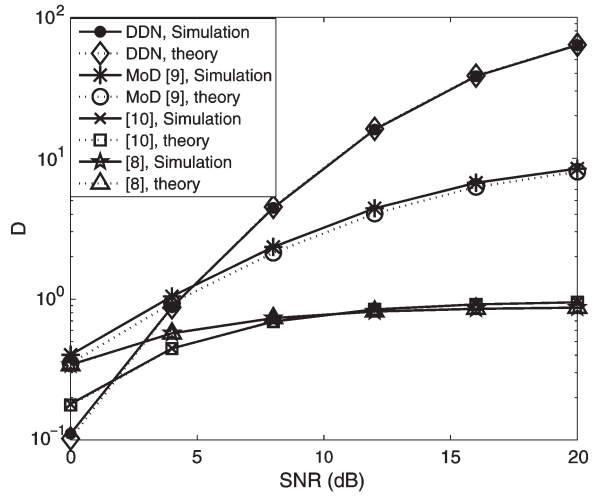

Fig. 7. Distance D comparing the class separability of the proposed DDN method obtained both theoretically and by simulations in the SUI-1 channel ($N = 256$ and $N_g = 16$).

3 dB. In this figure, the factor $\alpha_A^{\mathrm{CIDDN}}$ obtained by simulation is also drawn along with the theoretical lower bound in (38). Verified by the simulation results, the factor $\alpha_A^{\mathrm{CIDDN}}$, which compares the proposed CIDNN method with the method in [10], is independent of the correlation length (the curves are the same for all the correlation lengths) and shows the great performance improvement of the new method for all SNRs.

Fig. 7 shows distance D using both theory and simulation, where for the DDN method, we have $L = N/2$. It is observed that for SNR > 4 dB, the new method significantly increases the distance between the classes.

In Fig. 8, we have also shown distance D for the CIDDN method $(L = N/2)$ in comparison with the previous methods using simulation. According to this figure, for all SNRs, the proposed CIDDN method outstandingly increases the between-class distance. For example, at SNR ≥ 12 dB, the between-class distance of the proposed scheme is at least ten times

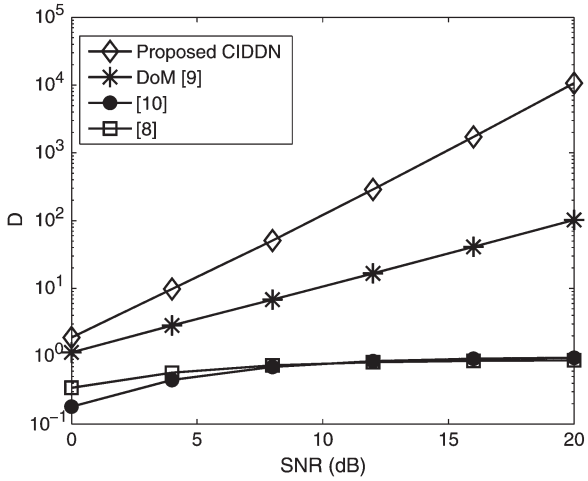

Fig. 8. Distance D comparing the class separability of the proposed CIDDN method obtained by simulations in the SUI-1 channel ($N = 256$ and $N_g = 16$).

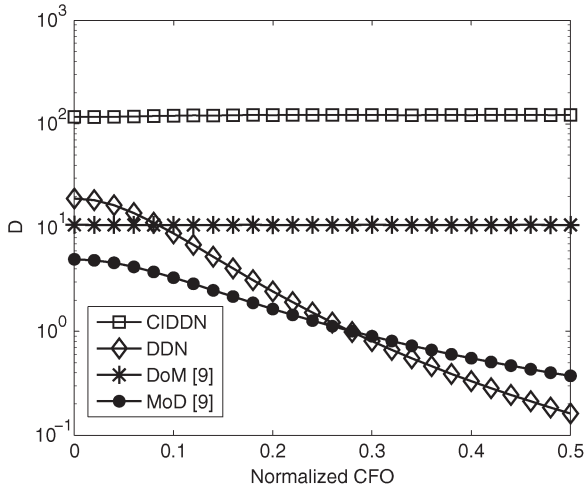

Fig. 9. Distance D for different values of CFO in the SUI-1 channel ($N = 256$ and $N_g = 16$).

higher than that in [9] and 100 times higher than those in [8] and [10].

The performances of different schemes for different values of normalized CFO are demonstrated in Fig. 9. As expected, the between-class distance for the proposed CIDDN method is not affected by the CFO, whereas the increase in the CFO reduces the class separability of the DDN method.

From the results previously obtained, it is observed that, sometimes, the proposed metrics do not have a good performance at low SNRs because (as mentioned in Section III) the new method has a greater peak at the correct timing instant for SNR > 3 dB and a smaller peak for SNR ≤ 3 dB (compared with [9]). Therefore, from the viewpoint of class separability, the smaller peak for SNR ≤ 3 dB can result in the reduction of the distance between the values of the new metric at correct and wrong timing points and, consequently, the reduction of class separability. However, note that the mean values of the proposed timing metrics at a wrong timing point inversely depend on the correlation length [as expressed in (20)]. Therefore, increasing the correlation length reduces the values

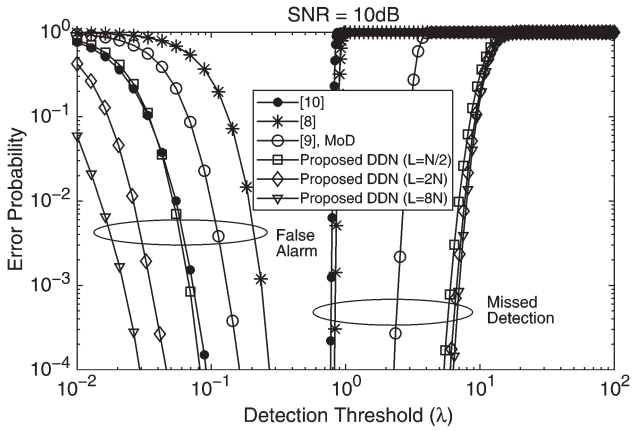

Fig. 10. Probabilities of false alarm and missed detection for the proposed DDN method in comparison with previous timing metrics in the SUI-1 channel at SNR $= 10$ dB ($N = 256$ and $N_g = 16$).

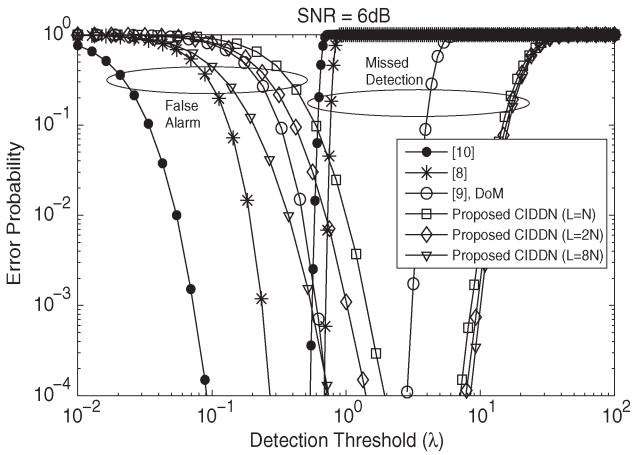

Fig. 11. Probabilities of false alarm and missed detection for the proposed CIDDN method in comparison with previous timing metrics in the SUI-1 channel at SNR $= 6$ dB ($N = 256$ and $N_g = 16$).

of the new metric at wrong timing points (compared with the previous methods), increases the class separability, and can compensate for the smaller peak at low SNRs. It is also worth mentioning that the SNR for many practical applications, as mentioned in [23], is SNR > 7 dB. For example, according to [24] and [25], the recommended SNR for the preamble is SNR $= 9.4$ dB.

We have shown false alarm and missed detection probabilities versus the detection threshold in Figs. 10–15. The probability of false alarm is the probability that at the wrong timing points (none of the samples belong to the preamble), the timing metric produces values higher than the specified threshold, and the MDP is the probability that at the correct timing point, the timing metric value falls below the threshold. Note that, in these figures, both axes are logarithmically depicted. This issue is particularly important when comparing the detection threshold, since the distances between thresholds (for example, the distance $0.1 \leq \lambda \leq 1$ and the distance $10 \leq \lambda \leq 100$) appear the same in the figures, but, in fact, they are not equal. This remark should be taken into account to avoid misinterpreting the threshold range in the figures.

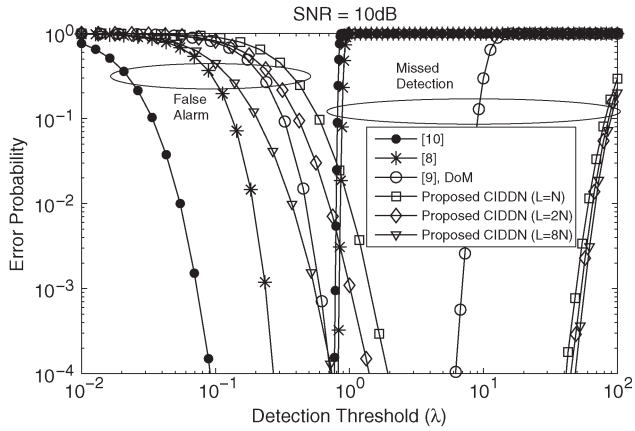

Fig. 12. Probabilities of false alarm and missed detection for the proposed CIDDN method in comparison with previous timing metrics in the SUI-1 channel at SNR $= 10$ dB ($N = 256$ and $N_g = 16$).

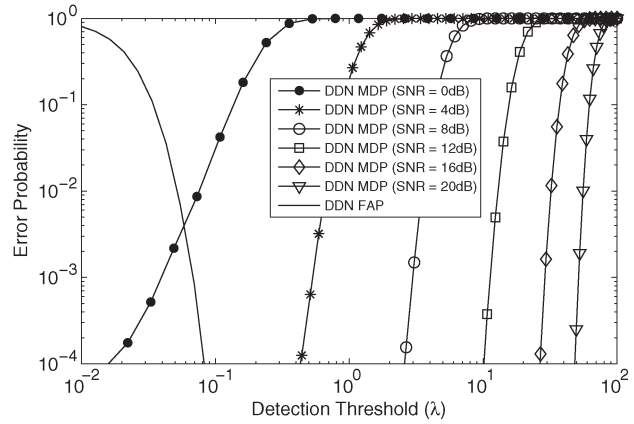

Fig. 13. MDP and false alarm probability (FAP) for the proposed DDN method for different values of SNR in the SUI-1 channel ($N = 256$, $N_g = 16$, and $L = N/2$).

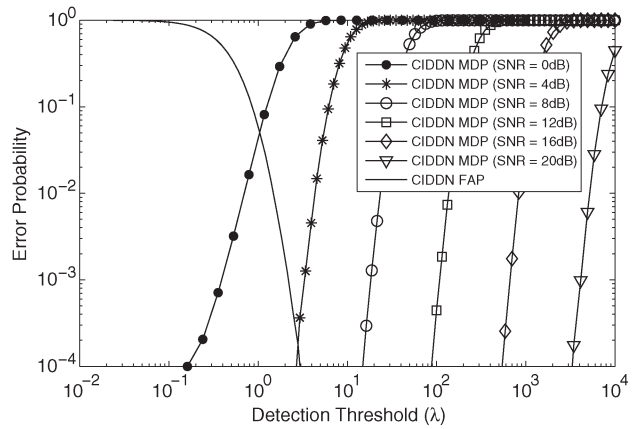

Fig. 14. MDP and FAP for the proposed CIDDN method for different values of SNR in the SUI-1 channel ($N = 256$, $N_g = 16$, and $L = N/2$).

In SNR $= 10$ dB, the false alarm and missed detection probabilities of the DDN metric and the previous metrics are manifested in Fig. 10, which shows the significant improvement of the proposed method in terms of the error probabilities and, consequently, the acceptable threshold range. For example, to have missed detection and false alarm probabilities lower than

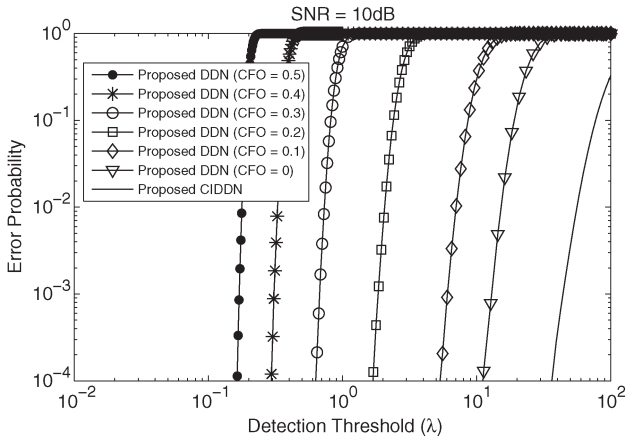

Fig. 15. Probabilities of missed detection for the proposed DDN and CIDDN methods for different values of CFO in the SUI-1 channel at SNR = 10 dB ($N = 256$, $N_g = 16$, and $L = N/2$).

10^{-3} for the proposed DDN method with $L = N/2$, the threshold can be chosen from the range $0.068 < \lambda < 6$, whereas this range is $0.072 < \lambda < 0.78$, $0.23 < \lambda < 0.84$, and $0.13 < \lambda < 2.3$ for the methods presented in [10], [8] and [9], respectively. It is concluded that the acceptable threshold range for the proposed DDN method is more than 7.5 times the acceptable threshold range for [10], more than 8.7 times the acceptable threshold range for [8], and nearly 2.5 times the acceptable threshold range for [9].

Fig. 11 compares the superior MDP performance of the proposed CIDDN method with the previous methods at SNR = 6 dB. In this figure, the probabilities of missed detection and false alarm less than 10^{-3} are obtained for the thresholds $1.4 < \lambda < 8.4$ for the proposed method at the correlation length of $L = N$ and for the thresholds $0.072 < \lambda < 0.55$, $0.23 < \lambda < 0.7$, and $0.6 < \lambda < 3.1$ for methods in [10], [8] and [9], respectively. This means that the CIDDN method widens the threshold range more than 14 times compared with those in [8] and [10] and 2.8 times compared with that in [9]. Furthermore, increasing the correlation length widens the range of thresholds of the new method.

In Fig. 12, the excellent performance of the proposed CIDDN method along with the performance of previous methods are demonstrated at SNR = 10 dB. According to this figure, the CIDDN scheme has a remarkably lower probability of missed detection and a slightly higher probability of false alarm. Thus, the CIDDN method has a considerably wider range of suitable thresholds. As an example, for $L = N$ and for the threshold in the range $1.4 < \lambda < 50$, the CIDDN method has false alarm and missed detection probabilities lower than 10^{-3}, whereas for the methods presented in [10], [8] and [9], these error probabilities occur for the threshold range $0.072 < \lambda < 0.78$, $0.23 < \lambda < 0.84$, and $0.6 < \lambda < 7$, respectively. In other words, the range of thresholds for error probabilities lower than 10^{-3} for the proposed method is more than 68 times that in [10], more than 79 times that in [8], and more than 7.5 times that in [9], respectively. These results demonstrate a huge improvement in the performance. It is worth mentioning that since the FAP does not depend on SNR [8]–[10], the FAP curves are the same in Figs. 11 and 12.

In Figs. 13 and 14, the probabilities of false alarm and missed detection of the proposed DDN and CIDDN methods for different values of SNR are shown, respectively. As it is observed, increasing SNR improves the performance of both methods.

Fig. 15 is dedicated to the missed detection probabilities of the proposed DDN and CIDDN methods for different values of CFO at SNR = 10 dB. According to this figure, increasing the value of CFO deteriorates the performance of the DDN method, whereas it does not have any effect on the performance of the CIDDN method. It is worth noting that we have not depicted the FAP because it is obtained when the preamble and, therefore, the CFO are not present.

VI. Conclusion

In this paper, the problem of timing synchronization in OFDM systems has been considered, and two novel timing metrics using differential normalization have been proposed. Based on two class-separability criteria, it was demonstrated that the new timing metrics, by taking advantage of the fourth-order statistics, improve the timing synchronization performance and result in timing metrics with sharper peaks. The complexity of the new normalization methods was investigated in comparison with that of the previous methods, and it was shown that by increasing the class separability, the new methods significantly improve missed detection and false alarm probabilities and offer considerably wider ranges of thresholds for frame detection.

Appendix

This Appendix is dedicated to the derivation of the mean values of CIDDN normalization function (23) at the correct and wrong instances. Without loss of generality, we consider $\left(Q^{\mathrm{CIDDN},d_{\mathrm{pr}}}(0)\right)^2$. At the correct timing point using (2) and (22), we have

$$\begin{aligned}
&\left(Q^{\mathrm{CIDDN},d_{\mathrm{pr}}}(0)\right)^2 \\
&\quad = \left(|r(d_{\mathrm{pr}})| - |r\left(d_{\mathrm{pr}} + (N/2)\right)|\right)^2 \\
&\qquad \times \left(|r(d_{\mathrm{pr}}+1)| - |r\left(d_{\mathrm{pr}} + (N/2) + 1\right)|\right)^2 \\
&\quad = \Bigg(\left| y(d_{\mathrm{pr}}) e^{j\frac{2\pi d_{\mathrm{pr}}}{N}\varepsilon} + w(d_{\mathrm{pr}}) \right| \\
&\qquad - \Bigg| y\left(d_{\mathrm{pr}} + (N/2)\right) e^{j\frac{2\pi\left(d_{\mathrm{pr}}+(N/2)\right)}{N}\varepsilon} \\
&\qquad\quad + w\left(d_{\mathrm{pr}} + (N/2)\right) \Bigg| \Bigg)^2 \\
&\qquad \times \Bigg(\left| y(d_{\mathrm{pr}}+1) e^{j\frac{2\pi(d_{\mathrm{pr}}+1)}{N}\varepsilon} + w(d_{\mathrm{pr}}+1) \right| \\
&\qquad - \Bigg| y\left(d_{\mathrm{pr}} + (N/2) + 1\right) e^{j\frac{2\pi\left(d_{\mathrm{pr}}+(N/2)+1\right)}{N}\varepsilon} \\
&\qquad\quad + w\left(d_{\mathrm{pr}} + (N/2) + 1\right) \Bigg| \Bigg)^2 . \qquad (47)
\end{aligned}$$

Considering that $y(d_{\rm pr}) = y(d_{\rm pr} + (N/2))$, we can rewrite the first term in (47) as

$$\begin{aligned}
&\left(\left|y(d_{\rm pr})e^{j\frac{2\pi d_{\rm pr}}{N}\varepsilon} + w(d_{\rm pr})\right|\right.\\
&\left.-\left|y(d_{\rm pr})e^{j\frac{2\pi(d_{\rm pr}+(N/2))}{N}\varepsilon}+w\left(d_{\rm pr}+(N/2)\right)\right|\right)^2\\
&=\left(\left|y(d_{\rm pr})e^{j\frac{2\pi d_{\rm pr}}{N}\varepsilon} + w(d_{\rm pr})\right|\right.\\
&\quad\left.-\left|e^{j\pi\varepsilon}\left(y(d_{\rm pr})e^{j\frac{2\pi d_{\rm pr}}{N}\varepsilon}+e^{-j\pi\varepsilon}w(d_{\rm pr}+(N/2))\right)\right|\right)^2\\
&=\left(\left|y(d_{\rm pr})e^{j\frac{2\pi d_{\rm pr}}{N}\varepsilon} + w(d_{\rm pr})\right|\right.\\
&\quad\left.-\left|e^{j\pi\varepsilon}\right|\left|y(d_{\rm pr})e^{j\frac{2\pi d_{\rm pr}}{N}\varepsilon}+e^{-j\pi\varepsilon}w\left(d_{\rm pr}+(N/2)\right)\right|\right)^2\\
&=\left(\left|y(d_{\rm pr})e^{j\frac{2\pi d_{\rm pr}}{N}\varepsilon} + w(d_{\rm pr})\right|\right.\\
&\quad\left.-\left|y(d_{\rm pr})e^{j\frac{2\pi d_{\rm pr}}{N}\varepsilon} + w\left(d_{\rm pr}+(N/2)\right)\right|\right)^2. \qquad (48)
\end{aligned}$$

In (48), multiplying $e^{-j\pi\varepsilon}$ and $w(d_{\rm pr} + (N/2))$ does not change the mean and variance of the noise term; hence, $e^{-j\pi\varepsilon}w(d_{\rm pr} + (N/2))$ is still a noise sample with the same mean and variance as $w(d_{\rm pr} + (N/2))$, and we can replace $e^{-j\pi\varepsilon}w(d_{\rm pr} + (N/2))$ with $w(d_{\rm pr} + (N/2))$ in (48). Similarly, the second term in (47) can be simplified as

$$\begin{aligned}
&\left(\left|y(d_{\rm pr}+1)e^{j\frac{2\pi(d_{\rm pr}+1)}{N}\varepsilon} + w(d_{\rm pr}+1)\right|\right.\\
&\left.-\left|y\left(d_{\rm pr}+(N/2)+1\right)e^{j\frac{2\pi(d_{\rm pr}+(N/2)+1)}{N}\varepsilon}\right.\right.\\
&\qquad\left.\left.+w\left(d_{\rm pr}+(N/2)+1\right)|\right|^2\right)^2\\
&=\left(\left|y(d_{\rm pr}+1)e^{j\frac{2\pi(d_{\rm pr}+1)}{N}\varepsilon} + w(d_{\rm pr}+1)\right|\right.\\
&\quad\left.-\left|y(d_{\rm pr}+1)e^{j\frac{2\pi(d_{\rm pr}+1)}{N}\varepsilon}+w\left(d_{\rm pr}+(N/2)+1\right)\right|\right)^2. \qquad (49)
\end{aligned}$$

Now, considering the triangle inequality for complex numbers x and y, i.e., $(|x| - |y|)^2 \le |x - y|^2$, and similar to [9], we have

$$\begin{aligned}
&\left(\left|y(d_{\rm pr})e^{j\frac{2\pi d_{\rm pr}}{N}\varepsilon} + w(d_{\rm pr})\right|\right.\\
&\quad\left.-\left|y(d_{\rm pr})e^{j\frac{2\pi d_{\rm pr}}{N}\varepsilon} + w\left(d_{\rm pr}+(N/2)\right)\right|\right)^2\\
&\le |w(d_{\rm pr}) - w\left(d_{\rm pr}+(N/2)\right)|^2 \qquad (50)\\
&\left(\left|y(d_{\rm pr}+1)e^{j\frac{2\pi(d_{\rm pr}+1)}{N}\varepsilon} + w(d_{\rm pr}+1)\right|\right.\\
&\quad\left.-\left|y(d_{\rm pr}+1)e^{j\frac{2\pi(d_{\rm pr}+1)}{N}\varepsilon} + w\left(d_{\rm pr}+(N/2)+1\right)\right|\right)^2\\
&\le |w(d_{\rm pr}+1) - w\left(d_{\rm pr}+(N/2)+1\right)|^2. \qquad (51)
\end{aligned}$$

Therefore

$$\begin{aligned}
&E\left\{\left(Q^{\rm CIDDN,d_{pr}}(0)\right)^2\right\}\\
&\quad\le E\left\{|w(d_{\rm pr}) - w\left(d_{\rm pr}+(N/2)\right)|^2\right\}\\
&\qquad\times E\left\{|w(d_{\rm pr}+1) - w\left(d_{\rm pr}+(N/2)+1\right)|^2\right\}\\
&\quad= 4\sigma_w^4. \qquad (52)
\end{aligned}$$

Consequently, we have

$$\begin{aligned}
E\left\{R^{\rm CIDDN}(d_{\rm pr})\right\} &= \sum_{k=0}^{L-1} E\left\{\left(Q^{\rm CIDDN,d_{pr}}(k)\right)^2\right\}\\
&= LE\left\{\left(Q^{\rm CIDDN,d_{pr}}(0)\right)^2\right\} \le 4L\sigma_w^4. \qquad (53)
\end{aligned}$$

At the wrong timing point, we have

$$\begin{aligned}
&E\left\{\left(Q^{\rm CIDDN,d_{ab}}(0)\right)^2\right\}\\
&= E\left\{\left(|r(d_{\rm ab})| - |r\left(d_{\rm ab}+(N/2)\right)|\right)^2\right.\\
&\qquad\left.\times\left(|r(d_{\rm ab}+1)| - |r\left(d_{\rm ab}+(N/2)+1\right)|\right)^2\right\}\\
&= E\left\{\left(|w(d_{\rm ab})| - |w\left(d_{\rm ab}+(N/2)\right)|\right)^2\right\}\\
&\qquad\times E\left\{\left(|w(d_{\rm ab}+1)| - |w\left(d_{\rm ab}+(N/2)+1\right)|\right)^2\right\}\\
&= \left(2-\frac{\pi}{2}\right)^2\sigma_w^4 \qquad (54)
\end{aligned}$$

which results in

$$\begin{aligned}
E\left\{R^{\rm CIDDN}(d_{\rm ab})\right\} &= \sum_{k=0}^{L-1} E\left\{\left(Q^{\rm CIDDN,d_{ab}}(k)\right)^2\right\}\\
&= LE\left\{\left(Q^{\rm CIDDN,d_{ab}}(0)\right)^2\right\}\\
&= \left(2-\frac{\pi}{2}\right)^2 L\sigma_w^4. \qquad (55)
\end{aligned}$$

REFERENCES

[1] S. H. Han and J. H. Lee, "An overview of peak-to-average power ratio reduction techniques for multicarrier transmission," *IEEE Wireless Commun.*, vol. 12, no. 2, pp. 56–65, Apr. 2005.

[2] T. M. Schmidl and D. C. Cox, "Robust frequency and timing synchronization for OFDM," *IEEE Trans. Commun.*, vol. 45, no. 12, pp. 1613–1621, Dec. 1997.

[3] H. Minn, M. Zeng, and V. K. Bhargava, "On timing offset estimation for OFDM systems," *IEEE Commun. Lett.*, vol. 4, no. 7, pp. 242–244, Jul. 2000.

[4] H. Minn, V. K. Bhargava, and K. B. Letaief, "A robust timing and frequency synchronization for OFDM systems," *IEEE Trans. Wireless Commun.*, vol. 2, no. 4, pp. 822–839, Jul. 2003.

[5] K. Shi and E. Serpedin, "Coarse frame and carrier synchronization of OFDM systems: A new metric and comparison," *IEEE Trans. Wireless Commun.*, vol. 3, no. 4, pp. 1271–1284, Jul. 2004.

[6] A. J. Coulson, "Maximum likelihood synchronization for OFDM using a pilot symbol: Algorithm," *IEEE J. Sel. Areas Commun.*, vol. 19, no. 12, pp. 2486–2494, Dec. 2001.

[7] A. J. Coulson, "Maximum likelihood synchronization for OFDM using a pilot symbol: Analysis," *IEEE J. Sel. Areas Commun.*, vol. 19, no. 12, pp. 2495–2503, Dec. 2001.
[8] M. Ruan, M. C. Reed, and Z. Shi, "Training symbol based coarse timing synchronization in OFDM systems," *IEEE Trans. Wireless Commun.*, vol. 8, no. 5, pp. 2558–2569, May 2009.
[9] J. Zhang and X. Huang, "Autocorrelation based coarse timing with differential normalization," *IEEE Trans. Wireless Commun.*, vol. 11, no. 2, pp. 526–530, Feb. 2012.
[10] H. Abdzadeh-Ziabari and M. G. Shayesteh, "Sufficient statistics, classification, a novel approach for preamble-aided frame detection in OFDM systems," *IEEE Trans. Veh. Technol.*, vol. 62, no. 6, pp. 2481–2495, Jul. 2013.
[11] H. Abdzadeh-Ziabari and M. G. Shayesteh, "Robust timing and frequency synchronization for OFDM systems," *IEEE Trans. Veh. Technol.*, vol. 60, no. 8, pp. 3646–3656, Oct. 2011.
[12] H. Abdzadeh-Ziabari and M. G. Shayesteh, "A novel preamble-based frame timing estimator for OFDM systems," *IEEE Commun. Lett.*, vol. 16, no. 7, pp. 1121–1124, Jul. 2012.
[13] G. Ren, Y. Chang, H. Zhang, and H. Zhang, "Synchronization methods based on a new constant envelope preamble for OFDM systems," *IEEE Trans. Broadcast.*, vol. 51, no. 1, pp. 139–143, Mar. 2005.
[14] J. Choi, J. Lee, Q. Zhao, and H. Lou, "Joint ML estimation of frame timing and carrier frequency offset for OFDM systems employing time-domain repeated preamble," *IEEE Trans. Wireless Commun.*, vol. 9, no. 1, pp. 311–317, Jan. 2010.
[15] W. L. Chin, "ML estimation of timing and frequency offsets using distinctive correlation characteristics of OFDM signals over dispersive fading channels," *IEEE Trans. Veh. Technol.*, vol. 60, no. 2, pp. 444–456, Feb. 2011.
[16] W. L. Chin, "Blind symbol synchronization for OFDM systems using cyclic prefix in time-variant and long-echo fading channels," *IEEE Trans. Veh. Technol.*, vol. 61, no. 1, pp. 185–195, Jan. 2012.
[17] S. Ma, X. Pan, G. H. Yang, and T. S. Ng, "Blind symbol synchronization based on cyclic prefix for OFDM systems," *IEEE Trans. Veh. Technol.*, vol. 58, no. 4, pp. 1746–1751, May 2009.
[18] V. Krishnamurthy, C. Athaudage, and D. Huang, "Adaptive OFDM synchronization algorithms based on discrete stochastic approximation," *IEEE Trans. Signal Process.*, vol. 53, no. 4, pp. 1561–1574, Apr. 2005.
[19] S. Theodoridis and K. Koutroumbas, *Pattern Recognition*, 4th ed. Amsterdam, The Netherlands: Elsevier, 2008.
[20] *(Amendment and Corrigendum to IEEE Std. 802.16-2004): IEEE Standard for Local and Metropolitan Area Networks Part 16: Air Interface for Fixed and Mobile Broadband Wireless Access Systems Amendment2: Physical and Medium Access Control Layers for Combined Fixed and Mobile Operation in Licensed Bands and Corrigendum 1*, IEEE Std. 802.16e-2005/IEEE Std. 802.16-2004/Cor 1-2005, 2006.
[21] V. Erceg *et al.*, "Channel models for fixed wireless applications," IEEE Task Group, Piscataway, NJ, USA, Tech. Rep IEEE 802.16a-03/01, Jul. 2003.
[22] G. M. van Kempen and L. J. van Vliet, "Mean and variance of ratio estimators used in fluorescence ratio imaging," *Cytometry*, vol. 39, no. 4, pp. 300–305, Apr. 2000.
[23] R. A. Pacheco, O. Üreten, D. Hatzinakos, and N. Serinken, "Bayesian frame synchronization using periodic preamble for OFDM-based WLANs," *IEEE Signal Process. Lett.*, vol. 12, no. 7, pp. 524–527, Jul. 2005.
[24] *Part 16: Air Interface for Fixed Broadband Wireless Access Systems*, IEEE Std. 802.16, 2004.
[25] C. H. N. Kishore and V. Umapathi Reddy, "A frame synchronization and frequency offset estimation algorithm for OFDM system and its analysis," *EURASIP J. Wireless Commun. Netw.*, vol. 2006, no. 1, p. 057018, Mar. 2006.

Ali Mohebbi received the B.S. degree in electrical engineering from Azad University of Karaj, Karaj, Iran, in 2006 and the M.S. degree in electrical engineering from Azad University, South Tehran Branch, Tehran, Iran, in 2011.

His research interests include ultrawideband radio communications, energy detection, and signal processing techniques for wireless communications, with focus on synchronization algorithms in orthogonal frequency-division multiplexing systems.

Hamed Abdzadeh-Ziabari (S'14) received the B.S. degree in electrical engineering from Azad University of Karaj, Karaj, Iran, and the M.S. degree in electrical engineering from Urmia University, Urmia, Iran. He is currently working toward the Ph.D. degree with Concordia University, Montreal, QC, Canada.

His research interests include statistical signal processing for wireless communication systems, including detection, estimation, and synchronization in orthogonal-frequency-division-multiplexing-based systems.

Mr. Abdzadeh-Ziabari received the Concordia University Full Tuition Recruitment Award.

Mahrokh G. Shayesteh (M'04) received the B.S. degree from the University of Tehran, Tehran, Iran; the M.S. degree from Khajeh Nassir University of Technology, Tehran; and the Ph.D. degree from Amir Kabir University of Technology, Tehran, all in electrical engineering.

She is currently an Associate Professor with Urmia University, Urmia, Iran. She is also working with the Wireless Research Laboratory, Advance Communications Research Institute, Department of Electrical Engineering, Sharif University of Technology, Tehran. Her research interests include wireless communication systems, spread spectrum, and image processing.